# Theoretical Insights into the Mechanism for Thiol/Disulfide Exchange

**Pedro Alexandrino Fernandes and Maria João Ramos*[a]**

**Abstract:** The mechanism for thiol/disulfide exchange has been studied with high-level theoretical calculations. Free energies, transition structures, charge densities, and solvent effects along the reaction pathway have been determined for the first time. Mechanistic results agree with experimental data, and support the idea that the thiolate is the reacting species and that the reaction indeed proceeds through an uncomplicated $S_N2$ transition state. The transition structures have the charge density evenly concentrated in the attacking and leaving sulfur atoms. The charge densities allow us to rationalize the solvent effects. As transition structures have the charge density more widely distributed than reactants, hydrophobic environments catalyze the reaction. The effect can be so dramatic that disulfide exchange inside the active site of ribonucleotide reductase is estimated to be catalyzed $10^3$ times faster than the reaction in water. It was also found that attack by thiol is much faster than previously assumed, if mediated through water chains. Although the present results, as well as experimental data, still suggest that thiolate is the main reaction species, water-mediated thiol attack is almost kinetically competitive, and can eventually become competitive under specific experimental conditions.

**Keywords:** ab initio calculations · density functional calculations · disulfide · mechanisms · sulfur

## Introduction

The thiol/disulfide exchange reaction is a biological fundamental process. This reaction can be represented schematically by the following set of chemical equations [Eqs. (1)–(4)]:

$$R{-}SH + H_20 \rightleftharpoons R{-}S^- + H_3O^+ \quad (1)$$

$$R{-}S^- + R'{-}SS{-}R' \rightleftharpoons R{-}SS{-}R' + R'{-}S^- \quad (2)$$

$$R{-}SS{-}R' + R{-}S^- \rightleftharpoons R{-}SS{-}R + R'{-}S^- \quad (3)$$

$$R'{-}S^- + H_3O^+ \rightleftharpoons R'{-}SH + H_2O \quad (4)$$

with the overall reaction being written as Equation (5):

$$2\,R{-}SH + R'{-}SS{-}R' \rightleftharpoons R{-}SS{-}R + 2\,R'{-}SH \quad (5)$$

The most abundant non-protein thiol in most cells is glutathione, and the glutathione/oxidized glutathione pair (G–SH/G–SS–G) forms the major intracellular redox buffer.[1,2] This buffer is responsible for maintaining the redox state of cells and for protecting the organism from oxidative stress. Thiol/disulfide exchange plays also an important role in the folding of proteins.[3,4] For proteins containing disulfide bonds, the folding rate is usually limited by a thiol/disulfide exchange reaction.[5] Many enzymes require a cysteine in their active site for catalysis: the thiol proteases,[6] enolase,[7] β-ketoacylthiolase,[8] and thioredoxin[9] are rendered inactive by the oxidation of the reactive thiol to a disulfide. Thiol–disulfide interchange has also been implicated as the triggering event in the cleavage of DNA by calichemicin and esperamicin.[10] Therefore, detailed knowledge about this reaction is needed for the interpretation of many biological phenomena.

In protein science it is fundamental to have a process of controlling the redox state of the cysteine groups. In the last five decades we have witnessed the development of reagents that can reduce/oxidize the proteins' disulfide bonds quickly and quantitatively.[11–18] Currently the most widely used reagent is dithiothreitol (DTT), which forms a very stable six-membered ring in the oxidized state, being an excellent reducing agent for proteins. However, this reagent is very expensive and effort has been made to find other reagents that can fulfill its role. The development of new reagents would be facilitated by the means to predict the structure of an "ideal" reducing agent. To be able to predict the reactivity of a thiol for disulfide exchange is a subject of intense re-

[a] Prof. P. A. Fernandes, Prof. M. J. Ramos
REQUIMTE/Faculdade de Ciências do Porto
Rua do Campo Alegre, 687, 4169-007 (Portugal)
Fax: (+35) 122-608-2959
E-mail: mjramos@fc.up.pt

Supporting information for this article is available on the WWW under http://www.chemeurj.org/ or from the author.

 **DOI: 10.1002/chem.200305343**  

search. Structure–activity relationships have been established for both aliphatic and aromatic thiols,[19–24] and it has been concluded that the reactivity of a thiol (and, hence, the kinetics of disulfide reduction) is mostly (but not only) determined by two opposite factors: the basicity and the nucleophilicity of the thiol group.[13,24] Hence, a thiol with a high p*K*a (e.g., 9.0) is expected to be a strong nucleophile, whereas one with a low p*K*a (e.g., 4–5) is expected to be a weak nucleophile. However, as the reacting species is believed to be the thiolate anion, low p*K*a thiols would be favored at physiological pH, as a larger fraction of anionic thiolate would be available to react. From the balance between these two factors it emerges that the most reactive thiols are those with a p*K*a close to the pH of the solution.[13,24]

The determination of the reaction mechanism has been the subject of investigation for a long time. Presently, it is believed that the thiolate anion is the reacting species. This conclusion is based on two principal arguments: the empirical knowledge that a protonated thiol is a weak nucleophile relative to a thiolate anion, and the experimental observation that the reaction is base-catalyzed when the thiol p*K*a is greater than the pH of the solution. pH-Dependent rate constants have been published before,[25–27] and an attempt to obtain pH-independent rate constants [i.e., rate constants for reactions in Eqs. (2) and (3), and not for the reaction in Eq. (5)] has been made. However, experimental data are somewhat dubious, because a good quantitative agreement between the independent rate constants measured at several pHs has not been obtained: independent rate constants can vary by 30–500% in a pH range of 0.7–2.9.[25,26] The best published results are those of Sheraga et al.,[27] but these were obtained with only three pH values in the range 7.5–8.7 (the rate constant decreases by only 5% in this interval). However, it is not fully understood to what extent this is a result of experimental uncertainty or whether it is a sign that something more complicated than a simple shift in the thiolate concentration is occurring. If we assume that the thiolate is the reacting species, then indirect evidence from experimental data suggest that the reactions should probably proceed through an uncomplicated $S_N2$ transition state.[19,22,23,28] Detailed and definitive knowledge of the chemical mechanism is crucial for the development of kinetically competent reducing agents, as well as to control the influence of solvent and other effects in the exchange kinetics. The geometry and charge distribution at the transition state, and all along the reaction coordinate are also fundamental to allow the rational design of new and more efficient reducing agents. Furthermore, this knowledge is also essential to understand the catalytic properties of disulfide formation/reduction or exchange of several enzymes, such as protein disulfide isomerase or thioredoxin.

To obtain new insights into the reaction we have conducted a series of high-level quantum mechanical calculations on the disulfide exchange mechanism. Several mechanistic alternatives were tested, and the results allow us to understand much better the amazing peculiarities of this reaction, and to rationalize the factors that can influence its kinetics.

## Computional Methods

Density functional theory was used in all calculations, with the Gaussian 98 suite of programs,[29] at the unrestricted Becke3LYP level of theory.[30–32] The 6–31G(d) basis set was used for geometry optimizations, and to calculate the zero-point, thermal, and entropic contributions. It is known that larger basis sets give very small additional corrections to the above properties, and their use is hence considered unnecessary from a computational view.[33–35] However, as we were dealing with a thiolate anion, the inclusion of diffuse functions could eventually have a measurable effect on geometries. Accordingly, we repeated some calculations using the 6–31G+(d) basis set in geometry optimizations. Sulfur–sulfur separations changed on average by only −0.003 Å. The only meaningful alteration was in the distance between the attacking and central sulfur atoms, which changed by −0.107 Å in the reactants. As this is only a weak nonbonding interaction, the potential-energy surface was very flat in that region, and changes in geometry tended to be large, although the corresponding changes in energy were very small (the overall differences were $+0.3\ \mathrm{kcal\,mol^{-1}}$ in the activation free energy and $+0.5\ \mathrm{kcal\,mol^{-1}}$ in the reaction free energy). The inclusion of diffuse functions also had a negligible effect on the sulfur atomic charges, which changed on average by only −0.004 a.u. The much larger 6—311+G(3df,2p) basis set was used to calculate the final electronic and solvation energies. This basis set was very close to saturation in the present system. The calculations were performed as follows: first, the transition states for each mechanistic step were located and optimized. Internal reaction-coordinate calculations, followed by further tighter optimizations, were performed to confirm which minima were connected to each transition state. Frequency analysis was performed at each stationary point on the potential-energy surface. Stationary points were characterized by the number of imaginary frequencies (none for minima and only one for transition states). A scaling factor of 0.9804 was used for the frequencies. Thermal and entropic effects were calculated at 298.15 K and added to the calculated energies.

As our system contained charged species, and the solvent (water) was highly polar, it was important to evaluate the influence of the solvent on the energetics. Moreover, $S_N2$ reactions are known to be solvent sensitive. Consequently, all energies were calculated under the influence of a dielectric continuum ($\varepsilon = 78.4$). For this purpose we used a polarized continuum model, called C-PCM, as implemented in Gaussian 98.[36] This method considers the solute as a set of interlocking spheres, centered on each atom, with apparent surface charges that interact with the wave function. The continuum is modeled as a conductor, instead of a dielectric. This simplifies the electrostatic computation, and corrections are made, a posteriori, for dielectric behavior. It is usually assumed that geometry optimizations can be carried out in vacuum and transferred to the continuum to calculate final energies, without introducing significant error.[37] This was indeed true for most reactions studied here, which have only a small energetic contribution from the continuum (i.e., differential contribution between reactants and transition states, or between reactants and products). However, the $S_N2$ reactions studied here have shown a large contribution from the continuum, and, hence, the geometries for the corresponding stationary points were re-optimized in the presence of the solvent.

The atomic charges are not an observable property, and, hence, the partitioning of the electronic density among atoms was always somewhat arbitrary. Thus, three different methods were used to calculate atomic charges, namely the Mulliken (Mull),[38] Merz–Kollman (MK)[39,40] and natural population analysis (NPA)[41–43] methods. Results were qualitatively equivalent, although some quantitative differences were observed.

## Results and Discussion

The disulfide exchange reaction occurs in two steps, represented by reactions (2) and (3). Despite qualitative changes in the electronic structure of the disulfides R′–SS–R′ and R–SS–R′ (due to the differences between R and R′, if any), reactions (2) and (3) are mechanistically equivalent. The rate for reaction (3) can be increased by using an attacking

dithiol instead of a simple thiol. However, the rate enhancement is not due to mechanistic considerations (like differences in the transition-state structure), but rather to the higher effective thiol concentration in the dithiol molecule. These reasons made us focus our attention on the mechanism for reaction (2), and take it as an general example for the disulfide exchange mechanism.

Small molecular models should be chosen if high-level theoretical results are to be obtained. The use of large models brings about the necessity of decreasing the theoretical level due to the enormous computing time needed to perform high-level calculations in large systems. Consequently, we have used methylthiol and ethylthiol as attacking nucleophiles. These molecules are good models for the widely used reducing agent 2-mercaptoethanol. They are also good models of cysteines. To model the disulfide we have used the most common protein reducing agent, dithiothreitol (DTT). Therefore, the model reaction consists of the nucleophilic attack of a methylthiol (in both protonated and anionic forms) to the disulfide bond of an oxidized DTT. Another reason for the use of the above mentioned models is that they are almost free of steric strain. It is well known that conformational strain plays an important role in disulfide exchange. However, DTT is almost free of steric strain due to the hexagonal ring formed in the oxidized state. The same occurs with methylthiol, for which no change in steric strain is expected when changing from the free thiolate to the covalent product. Activation and reaction energies obtained with these molecules will reflect, therefore, the intrinsic chemistry of the reaction, as they have no significant contribution from stereochemical strain.

**Nucleophilic attack by methylthiolate along the S–C DTT bond**: In an earlier study, 72 crystalographic structures of organic, inorganic, and organometalic compounds containing divalent sulfur (i.e., sulfur bound to two ligands, neither one being H) have shown that the preferred orientation for nucleophilic attack is along one of the two sulfur bonds.[44] Based on these results, we have studied the reaction with the thiolate attacking along both the S–C and S–S bonds. It should be noted that the LUMO orbital of DTT has main contributions from the two sulfur atoms, and is directed along the S–S bond. Therefore, it is expected that addition along the direction of the S–S bond is favored. However, and to begin with, results for the attack along the S–C bond are discussed. The reaction is shown schematically in Scheme 1 below.

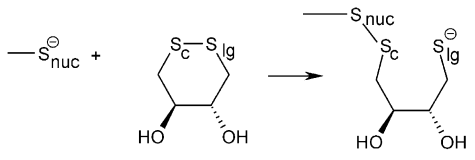


Scheme 1. Nucleophilic addition of methiolthiolate to DTT.

The nucleophilic sulfur has been named $S_{nuc}$, the central sulfur $S_c$, and the leaving sulfur $S_{lg}$. The transition state is shown in Figure 1A.

The transition structure is characterized by S–S bonds that have intermediate lengths between a disulfide bond and a thiol–disulfide interaction ($S_{nuc}$–$S_c$ = 2.58 Å and $S_c$–$S_{lg}$ = 2.88 Å). The difference in length between $S_{nuc}$–$S_c$ and $S_c$–$S_{lg}$ can in part be attributed to the asymmetry of the molecular system. In the reactants, the disulfide bond is 2.10 Å and the $S_{nuc}$–$S_c$ separation was 3.18 Å. In the products, the new disulfide bond has a length of 2.09 Å and the $S_c$–$S_{lg}$ length increased to 4.78 Å. The charge has also been transferred from $S_{nuc}$ to $S_{lg}$ along the reaction pathway (see Figure 1A). At the transition state the charge density is delocalized between the two peripherical sulfur atoms, being more concentrated at $S_{lg}$ and almost zero at $S_c$. The gas-phase free-energy barrier was calculated to be 26.7 kcal mol$^{-1}$, and the reaction free energy to be −12.6 kcal mol$^{-1}$. As disulfide exchange is mostly important in aqueous media, we have recalculated the free-energy barrier and reaction free energy from the thermodynamic cycle shown below by the relationship given in Equation (6), whereby $\Delta\Delta G_{solv}$ is given by Equation (7).

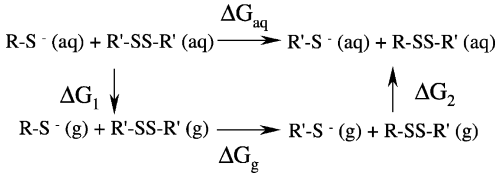


$$\Delta G_{aq} = \Delta G_g + \Delta\Delta G_{solv} \quad (6)$$

$$\Delta\Delta G_{solv} = \Delta G_1 + \Delta G_2 = \Delta^{Prod}_{solv} - \Delta^{React}_{solv} \quad (7)$$

Accurate experimental kinetic and equilibrium constants for several thiol/disulfide exchange reactions are available in the literature.[18,20,21,23,25–27,29,33,34,45–47] Although data for the compounds used here are not available, there are data for many similar thiol/disulfide systems, from which we can expect the reaction free energy to be close to zero and the free-energy barrier to be approximately 14.4–15.8 kcal mol$^{-1}$ (transition-state theory extrapolation from typical pH-independent thiolate rate constants of $10^3$–$10^4$ M$^{-1}$ min$^{-1}$ for disulfide exchange between aliphatic thiols similar to the ones considered here). However, the solvent contribution increased the free-energy barrier further to 43.4 kcal mol$^{-1}$, which is far beyond typical experimental values. This effect is due to a preferential stabilization of the reactants over the transition state. Indeed, in the reactants the charge density is concentrated in the methylthiolate, whereas in the transition state it is much more delocalized through the peripheral sulfur atoms. As water is a highly polar solvent, it will stabilize further the more polar solutes. Moreover, the area exposed to the solvent is larger for the reactants than at the transition state, resulting in a larger hydration number for the thiolate in the reactants.

The free energy of reaction in solution corresponds to −0.7 kcal mol$^{-1}$, which is what would be expected from an inherently thermoneutral reaction. The conclusion is that a mechanism involving addition of a nucleophile along the

  

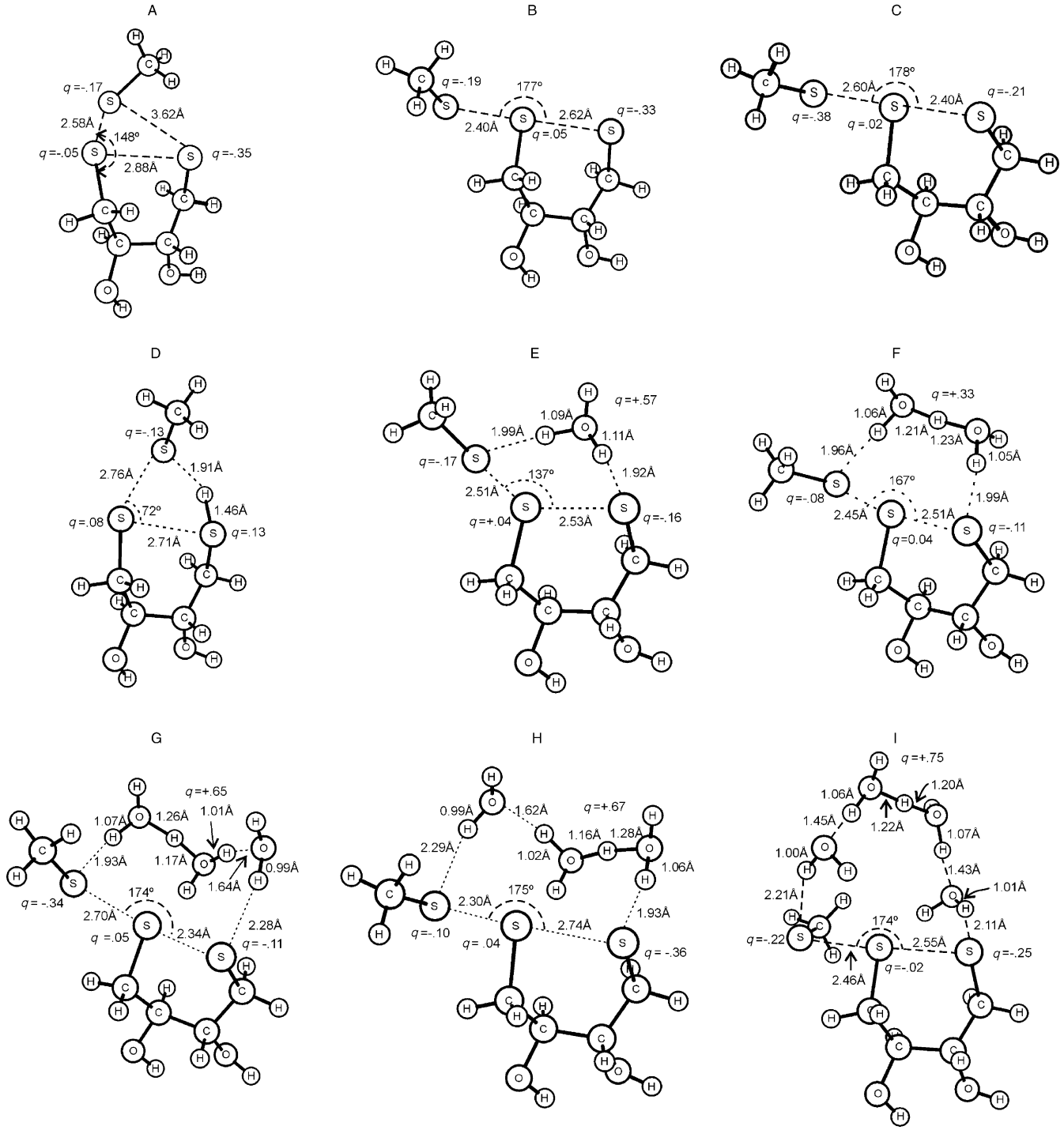


Figure 1. Some of the most relevant stationary points discussed in the text. A) Transition state for thiolate attack along the S–C bond. B) Trisulfide anion in the gas phase. C) Transition state for $S_N2$ thiolate attack in water. D) Transition state for (protonated) thiol attack. E)–I) Transition states for thiol attack, mediated by one (E), two (F), three (G and H) and four (I) water molecules. Important distances (Å), angles (degrees), and charges (a.u., NPA method) are shown.

S–C bond is inconsistent with experimental kinetics and should thus be excluded.

**Nucleophilic attack by ethylthiolate along the S–C DTT bond**: We decided to perform some additional tests to check the computational accuracy of the results obtained. The first deals with the models used. As methylthiol is truncated too close to the sulfur atom, we repeated the calculations using ethylthiol. The results were equivalent: the geometry of the common part of both systems was the same within computational accuracy. Sulfur atomic charges were also almost equivalent (average difference of 0.002 a.u.), except for $S_{nuc}$,

whereby inductive effects caused by the ethyl group decreased the charge by an average of 0.12 a.u. This last difference is small, even though not negligible, but the final energies obtained with methylthiol and ethylthiol were still almost equivalent (differences of $+0.2$ and $-0.6$ kcal mol$^{-1}$ in the activation and reaction free energies, respectively).

**Nucleophilic attack by methylthiolate along the S–C DTT bond—geometry optimization in the continuum**: Another test deals with the influence of transferring gas-phase optimized geometries to aqueous solution. This can usually be done without introducing significant error. However, in this reaction the contribution from the solvent to the free energy is very large ($\Delta\Delta G_{solv} = 16.5$ kcal mol$^{-1}$ is the free-energy barrier), and thus the solvent plays a key role in the reaction. Therefore, we re-optimized the stationary points in the presence of the continuum. This is a very difficult calculation, as geometry optimizations of ionic species in water are always very difficult. The structures obtained were very similar to the gas-phase ones. The only meaningful difference was that in the reactants the distance between the thiolate and the disulfide increased to 6.96 Å, to allow for a more extensive solvation of the thiolate. Thiolate solvation decreased the energy of the reactants and increased the barrier from 43.5 to 49.0 kcal mol$^{-1}$, which is a small but significant difference. The energies obtained are still too high compared with experimental values; this suggests that this is not the correct mechanism for thiol/disulfide exchange.

**Nucleophilic attack by methylthiolate along the S–S DTT bond in the gas phase**: We proceeded by investigating a similar $S_N2$ mechanism, with the nucleophilic attack being performed along the S–S bond. We started by performing a scan along $S_{nuc}$–$S_c$. Surprisingly, the only stationary point found corresponds to the $[R\text{-}S_{nuc}\text{-}S_c\text{-}S_{lg}\text{-}R_2']^-$ trisulfide anion shown in Figure 1B, with both S–S bonds having intermediate lengths between a single bond and a nonbonding contact. This stationary point was confirmed to be a minimum by analytic calculation of the Hessian. This is not, however, the absolute minimum for the complex. The latter has both the hydroxyl groups of DTT forming hydrogen bonds to the thiolate sulfur. The difference in energy between these minima amounts to 13.9 kcal mol$^{-1}$. This means that the stationary point corresponding to the trisulfide anion will not be populated at room temperature.

The existence of trisulfide anions has been studied before. Pioneering gas-phase theoretical studies support the existence of stable $R_3S_3^-$ ions considered to be possible intermediates during disulfide exchange.[48] However, later ab initio calculations at the HF/6–31G(d) level identified a similar stationary point as a transition state (with a vibrational frequency of 218i cm$^{-1}$), located 14.37 kcal mol$^{-1}$ above the dithiol/thiolate complex.[49] This transition state was thus proposed as the one for the gas-phase thiol/disulfide exchange reaction.

Our results support the first early study, and are in disagreement with the second. At the B3LYP6–31G(d) level the structure in Figure 1B is indeed a minimum, and not a transition state. Thus, it seems that to neglect electron correlation led to such a distortion on the potential-energy surface that it even changed the nature of the stationary point (from a minimum to a transition state).

We conclude that the trisulfide anion is a minimum in the gas-phase potential-energy surface, but its high energy relative to the global minimum rules out its existence as a stable species. However, it is known that in solution the picture can be quite different as anionic species are highly stabilized by polar solvents. Moreover, $S_N2$ reactions are known to be solvent sensitive. Consequently, we have conducted a study for the same reaction, but now, for the first time, in water.

**Nucleophilic attack by methylthiolate along the S–S DTT bond in water**: We started by performing a scan along the $S_{nuc}$–$S_c$ coordinate in the presence of a dielectric continuum. The results confirm our expectations: the solvent does not just influence the reaction, it fully determines which reactants and products will exist. We have depicted in Figure 2 the electronic energy in the gas phase and in water along the reaction coordinate.

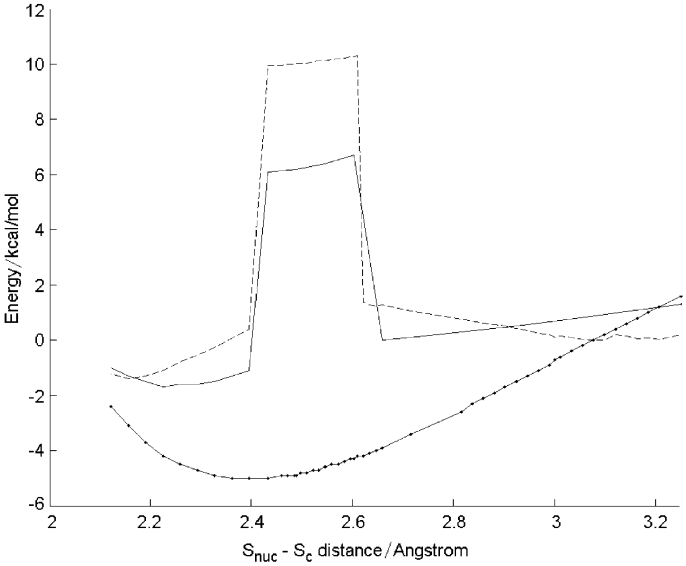


Figure 2. Scan along the $S_{nuc}$–$S_c$ bond in the gas phase (dotted line), in water (dashed line), and in the active site of RNR (solid line). Distances (Å) and energies (kcal mol$^{-1}$) are given. The dots correspond to the points calculated during the scan.

The scale for the electronic energy has been shifted 65 kcal mol$^{-1}$ below, in order to represent all three lines on the same graph. This confirms the existence of the single minimum depicted in Figure 1B. However, inclusion of the solvent completely changes the shape of the potential-energy surface. Both reactants and products can be identified in water. The geometries for the transition state, reactants, and products were taken from the scan and were further optimized in the continuum without constraints. The transition structure obtained for the $S_N2$ reaction in water has an $S_{nuc}$–$S_c$ distance of 2.61 Å and $S_c$–$S_{lg}$ distance of 2.47 Å, and is depicted in Figure 1C. Including thermal and entropic effects and recalculating the stationary points with

  

the 6—311+G(3df,2p) basis set, we obtain a final free-energy barrier of 14.8 kcal mol$^{-1}$ and a final reaction free energy of 1.8 kcal mol$^{-1}$.

These results are in excellent agreement with the thermodynamic and kinetic experimental data. The reaction is almost thermoneutral, as should be expected, and the free-energy barrier (14.8 kcal mol$^{-1}$) lies well within the typical experimental values of 14.4–15.8 kcal mol$^{-1}$.

These results strongly support and confirm the hypothesis that thiol/disulfide exchange proceeds through an uncomplicated $S_N2$ transition state. Moreover, this seems to be the first unambiguous and definitive assignment of a mechanism for disulfide exchange in water, since earlier experimental suggestions were always based on indirect evidence.[19,22,23,28]

Figure 3 shows the atomic charges for the three sulfur atoms along the $S_{nuc}$–$S_c$ coordinate, calculated by the NPA method. All three MK, NPA, and Mull methods give identical qualitative results. MK charges tend to be slightly larger.

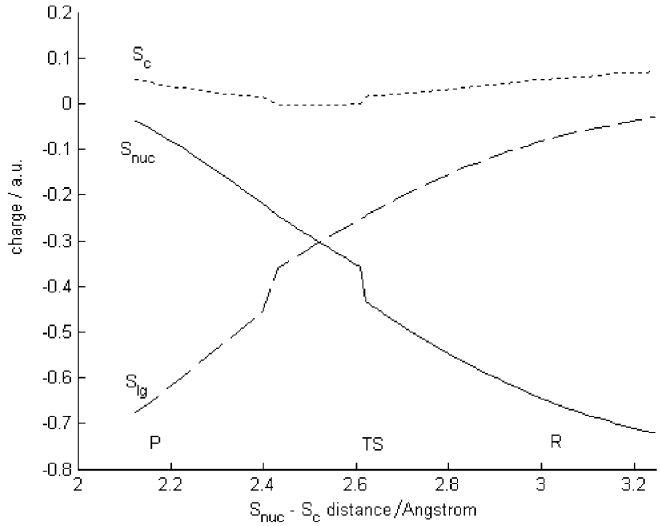


Figure 3. Atomic charges (a.u.) for $S_{nuc}$ (solid line), $S_c$ (dotted line) and $S_{lg}$ (dashed line) calculated by NPA method.

The results allow us to prove earlier proposals derived from experimental Brønsted relations between the reaction rate and the p*K*a of the conjugated thiol. From these and other data it was concluded that the peripheral sulfur atoms should have significant negative charge at the transition state, with a zero or a small negative charge at the central sulfur atom.[19,22,50–52] Earlier theoretical studies have also assigned most charge to the peripheral sulfur atoms in the $H_3S_3^-$ ion, and a small positive charge to the central one (−0.62 and +0.02 a.u., respectively).[48] Moreover, the results obtained here show that this picture holds along all of the reaction coordinate, and not only at the transition state (except for the central sulfur atom, where the charge is always very small, but can be eventually positive). Therefore, we can conclude that along the reaction pathway the charge is transferred directly from $S_{nuc}$ to $S_{lg}$ without accumulating at $S_c$.

This picture allows us to rationalize the effect of the solvent: the solvent stabilization will be at a maximum at the end points of the reaction coordinate, where charge is mostly concentrated on $S_{nuc}$ or $S_{lg}$, and will decrease to its minimum at the transition state region, where the charge is more evenly distributed. The greater the polarity of the solvent, the larger the stabilization of the reactants will be in relation to the transition state. This behavior has extensive chemical precedents, as $S_N2$ reactions between neutral and charged species are usually slowed down in polar solvents. Thus, polar environments increase the activation energy, slowing down the reaction, and nonpolar hydrophobic environments decrease the barrier, catalyzing the reaction. This is an important result for protein science, as it points out a way in which proteins can catalyze disulfide exchange: by providing a hydrophobic environment.

Some examples can be given: protein disulfide isomerase (PDI, E.C. 5.3.4.1) is the in vivo catalyst for disulfide isomerization, and consequently for protein folding of disulfide-containing proteins.[53–63] PDI is a 55 kDa protein with two active sites, each with a pair of cysteines in the sequence WCGHCK.[63] In each active site one of the cysteine thiols has an abnormally low p*K*a ($C_{nuc}$, p*K*a = 6.7[54]) and is exposed to the solvent, and the second cysteine thiol is protected from the solvent and has a normal p*K*a ($C_{rescue}$, p*K*a ca. 9.0).[54] The cysteines form a disulfide bond when PDI is in the oxidized form. The working mechanism for disulfide isomerization of misfolded disulfide-containing proteins begins with addition of $C_{nuc}$ to a non-native disulfide, resulting in a PDI–substrate covalent complex. The reduced substrate thiol then scans the substrate for other unstable disulfides, reacting with it. This intramolecular rearrangement ends with addition of a substrate thiol to the crossed PDI–substrate disulfide, thus releasing PDI for a new catalytic cycle (Scheme 2, pathway I). If the reduced substrate thiolate takes too long to find reactive disulfides the enzyme becomes trapped in the covalent complex, and consequently will be unavailable to catalyze further disulfide isomerizations. However, both the second cysteine ($C_{rescue}$) and the redox buffer can act as rescue systems (molecular clocks), by adding to $C_{nuc}$ with consequent release of PDI from the covalent complex (Scheme 2, pathways II and III, respectively), and leaving one more reduced thiolate ready for scanning for reactive non-native disulfides.[58,59,62]

Experimental data on the isomerization of scrambled RNase assisted by PDI show that the dominant mechanism for PDI release corresponds to addition of $C_{rescue}$ to $C_{nuc}$ (pathway II) rather than addition of a buffer or protein thiolate (pathways III and I).[59] Escape assisted by the redox buffer is only meaningful in PDI mutants lacking $C_{rescue}$. Moreover, enzymes with $C_{rescue}$ mutated to a serine accumulate in covalent complexes with the substrate, especially in the absence of a redox buffer, and have reduced isomerization activity.

The reason why the dominant pathway for disulfide rearrangement towards the native structure is pathway II can be understood by considering the results obtained here. As the PDI–substrate disulfide is exposed to the solvent, and $C_{rescue}$ is instead located in a hydrophobic pocket, we can predict

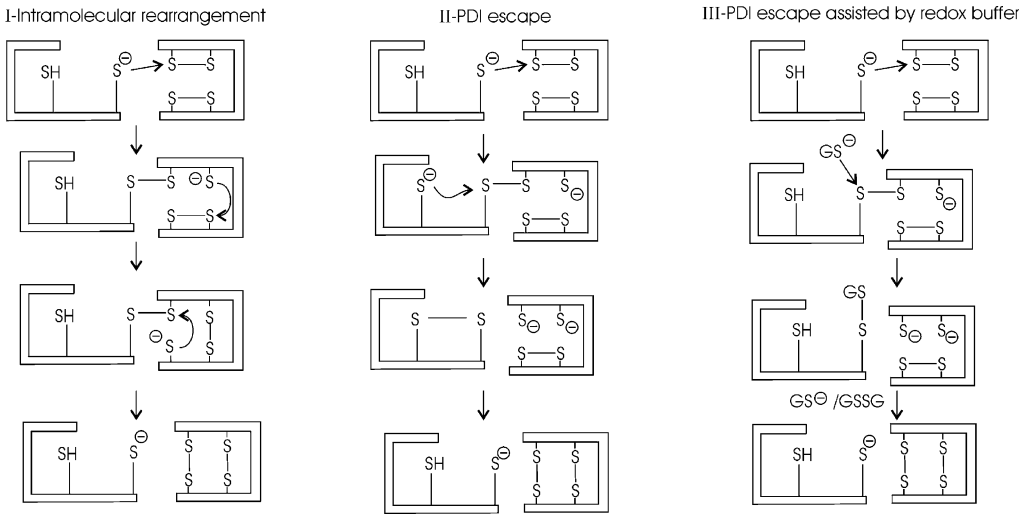


Scheme 2. Mechanism for disulfide isomerization. The release of PDI from the covalent enzyme–substrate complex can be accomplished by addition of I) a substrate thiolate; II) $C_{rescue}$; III) a thiol from the redox buffer.

that addition of the buried $C_{rescue}$ to the disulfide will be the kinetically faster pathway to release PDI from the covalent complex for a new turnover. Both the higher effective disulfide concentration in PDI (compared to the redox buffer) and the lowering of the free-energy barrier due to the hydrophobic environment mentioned above contribute to this.

Our results allow us to propose an additional role for the large hydrophobic PDI region beyond the active site. This large nonreactive region has been demonstrated to be important for catalytic activity. It was proposed that its function is both to catalyze conformational changes in the folding substrate and to bind the substrate (the protein binds preferentially unfolded substrates).[54,60,61,64,65] We propose here that another function for this region should be to provide a hydrophobic environment to the superficial region of the folding substrate upon binding. This will lower the free-energy barrier for thiol/disulfide exchange between surface thiolates and disulfides, and will consequently catalyze the intramolecular rearrangement of the non-native disulfide bonds.

To estimate the influence of the environment on the rate constant, we have recalculated the scan along the $S_{nuc}$–$S_c$ coordinate using a dielectric constant of 4 (Figure 2). This value is adequate for the active site of the enzyme ribonucleotide reductase, in which a disulfide exchange reaction takes place.[66] As expected, the free-energy barrier is lowered by 4 kcal mol$^{-1}$, corresponding to a $10^3$ increase in the rate constant (see Figure 1).

**Thiol attack along the S–S bond in water**: To identify the reaction above beyond doubt as an $S_N2$ mechanism for disulfide exchange, we decided to check whether nucleophilic attack by a protonated thiol is indeed as unfavorable as it is usually considered. Although it is evident that a protonated thiol is a weak nucleophile relative to thiolate, we must keep in mind that the hydration of a thiolate anion is far more favorable than the hydration of a neutral thiol. Therefore, the solvent will stabilize the reagents much more than the corresponding transition state, increasing the barrier to thiolate attack. We should thus determine to what extent this reactant stabilization is compensated by the increased nucleophilicity of the thiolate anion. The transition state for thiol attack is depicted in Figure 1D. The thiol proton is transferred to $S_{lg}$ with concerted addition of $S_{nuc}$ to $S_c$. However, this kind of concerted step forces the attacking thiol to deviate markedly from the direction of the attack (from an S-S-S angle of about 180° to an angle of 77°), which makes the reaction rather unfavorable, with an activation energy of 61.0 kcal mol$^{-1}$. Thus, this reaction can be ruled out.

**Thiol attack along the S–S bond in water catalyzed by water chains**: To facilitate the attack of the protonated thiol we subsequently performed the reaction mediated by water molecules, which forms a water chain with the tails connected to both the $S_{nuc}$ and the $S_{lg}$ atoms. The proton is transferred through the water chain simultaneously with the attack of the nascent thiolate to $S_c$. Such a reaction can be viewed as a concerted deprotonation of the attacking thiol, attack of the in situ-generated thiolate to the disulfide bond, and protonation of the leaving thiolate. In summary, it corresponds to a coupling of reactions (1), (2), and (4), through a single transition state. The advantage of this mechanism would be that the thiolate is generated during the reaction, and thus the thiolate stabilization by the solvent becomes less important. Moreover, it will allow linear S-S-S addition if enough water molecules are incorporated in the chain, and will use the most abundant (protonated) thiol species at physiological pH to carry out the reaction. The transition states for such reactions with one, two, three, and four water molecules are depicted in Figure 1E, F, G, H, and I. It should be stressed that no significant entropic cost is expected in order to obtain the transition-state structures in aqueous environment, as the thiol and the disulfide are fully surrounded by water molecules.[67] Therefore, the water chains

  

are indeed already, and always, present. Moreover, the pictures show only some of the possible pathways for proton transfer through the solvent and others can eventually exist with lower activation energies. The transition states share a common pattern: all of them have a charge separation, with a positive charge located at the water chain and a negative charge delocalized between the two peripheral sulfur atoms (again zero at the central sulfur). The larger the number of water molecules the closer the S-S-S angle to linearity. The inclusion of a single water molecule does not lead to a significant lowering of the free-energy barrier; only water chains with at least two water molecules are efficient. For these, the resulting activation energies (27–34 kcal mol$^{-1}$, see Table 1) are much lower than that for direct thiol attack, but they are still higher than for the thiolate attack. However, some corrections should be made; it is known that a dielectric continuum gives poor results when water molecules are explicitly included in the model.[67] Controversially, the consideration of explicit hydrogen bonding to the water chain should be important in this case, although that approach is impracticable even with very generous computer resources. Probably the best way to account for all such corrections is to take advantage of the reliable experimental data on the kinetics for proton exchange between cysteine thiols and water. Siegbahn and co-workers have calculated such transition states at a similar theoretical level.[67] The reaction is quite similar to the one proposed here, with the difference that both tails of the water chain are hydrogen bonded to the same instead of different sulfur atoms The structures for both transition states are otherwise very similar. These corrections already account for the limitations of the continuum, as well as from the theoretical method itself, as they are intended to reproduce experimental results. Upon adding up such corrections for the most favorable transition state (−5.5 kcal mol$^{-1}$, for three water molecules) the activation free energy is reduced to 22.0 kcal mol$^{-1}$.

Moreover, we must keep in mind that the thiol/thiolate ratio is about $10^2$ at physiological pH, which should compensate for approximately 2.8 kcal mol$^{-1}$ of the difference in the free-energy barrier for thiol attack, when compared to the one for the thiolate attack. The overall difference between the experimental barrier for the $S_N2$ thiolate mechanism (14.4–15.8 kcal mol$^{-1}$) and the values calculated here for the thiol attack mechanism mediated by water chains reduces to 3.4–4.8 kcal mol$^{-1}$, which is by far lower than anyone could have expected. Such water-chain-mediated disulfide exchange should in principle exhibit a similar structure–reactivity relationship to the thiolate attack, as its kinetics will still depend on the nucleophilicity of the thiolate anion generated (in situ) and on the p*K*a of the thiol (that will be deprotonated anyway). The conclusion is that although the thiolate addition is still the dominant mechanism here, the concept of a concerted deprotonation/substitution/protonation reaction mediated by water chains should not be definitively excluded solely based on a single chemical reaction performed in a single chemical environment. This kind of mechanism can in principle be applied to any $S_N2$ reaction in which the leaving and attacking groups are weak bases.

Table 1. Activation and reaction free energies ($\Delta G_{act}$ and $\Delta G_r$, respectively) for all the mechanisms discussed. Electronic energies and contributions from the continuum were calculated at the B3LYP6—311++G(3df,2p)//B3LYP6–31G(d) level of theory. Remaining terms were calculated at the B3LYP6–31G(d)//B3LYP6–31G(d) level of theory. The energy is separated into contributions from the electronic energy ($E_{el}$), zero-point energy (ZPE), Thermal energy ($E_{thermal}$), entropic contribution ($-T\Delta\Delta S$) and contribution from the solvent ($\Delta\Delta G_{solv}$). The last column shows the reaction free energy.

| Mechanism[a] | $\Delta G_{act}$ | $E_{el}$ | ZPE | $E_{thermal}$ | $-T\Delta\Delta S$ | $\Delta\Delta G_{solv}$ | $\Delta G_r$ |
|---|---|---|---|---|---|---|---|
| $CH_3S^-$ (SSC) | 43.4 | 24.4 | −0.2 | −0.6 | 2.9 | 16.8 | −0.7 |
| $CH_3S^-$ (SSC) (diff. fn.)[b] | 43.6 | 26.5 | −0.2 | −0.6 | 2.9 | 15.0 | −0.2 |
| | 43.5 | 25.8 | −0.2 | −0.5 | 1.9 | 16.5 | −1.3 |
| $CH_3CH_2S^-$ (SSC) | | | | | | | |
| | 49.0 | 21.9 | −0.4 | 0.0 | 1.6 | 26.0 | 5.4 |
| $CH_3S^-$ (SSC) + solvent[c] | | | | | | | |
| | 14.8 | −15.7 | −0.6 | 0.1 | 1.1 | 29.9 | 1.8 |
| $CH_3S^-$(SSS) + solvent | | | | | | | |
| | 61.0 | 64.1 | −2.0 | −0.7 | 3.9 | −4.2 | 3.8 |
| $CH_3SH$ | | | | | | | |
| | 52.0 | 50.1 | −1.2 | −1.6 | 6.8 | −2.1 | 5.7 |
| $CH_3SH + 1H_2O$[d] | | | | | | | |
| $CH_3SH + 2H_2O$[d] | 33.2 | 30.1 | −1.2 | −1.9 | 6.9 | −0.74.6 | |
| $CH_3SH + 3H_2O$[d] | 27.5 | 23.4 | 0.9 | −1.4 | 5.9 | −1.4 | 4.5 |
| $CH_3SH + 4H_2O$[d] | 34.2 | 29.5 | −0.6 | −2.2 | 6.8 | 0.7 | 5.3 |
| Exptl. ($K_v = 10^3$–$10^4$ M$^{-1}$ min$^{-1}$) | 14.4–15.8 | – | – | – | – | – | – |

[a] SSS and SSC indicate the direction for thiolate attack. [b] Geometry optimization with the 6—31+G(d) basis set. [c] Geometry optimization in the presence of the solvent. [d] Before correction.

## Conclusions

This work was devoted to the study of the mechanism for disulfide exchange in water. Several mechanistic alternatives have been explored, and the results compared with the available experimental data. In Table 1 we have summarized the energetic results.

The earlier hypothesis that disulfide exchange should proceed through an uncomplicated $S_N2$ transition state has been demonstrated here. This is the most favorable mechanism from a kinetic point of view, and is the only one in which theoretical results give excellent agreement with the observed kinetics. The results in Table 1 also show that the difference in activation energy between the experimental value and all other alternative mechanisms is well beyond the accuracy of the theoretical method (~3 kcal mol$^{-1}$), reinforcing the conclusions.

A correct transition structure has been determined for the first time, as well as the atomic charges for the three sulfur atoms along the reaction coordinate. The earlier proposals

for the charge distribution at the transition state charge have been confirmed. Moreover, it has been shown that charge is transferred all along the reaction pathway, from the attacking to the leaving sulfur atoms without ever accumulating at the central sulfur. The effect of the solvent has been rationalized, and it was concluded that hydrophobic environments catalyze the reaction. Implications for protein folding and for enzymatic disulfide exchange have been discussed: as an example it was found that disulfide exchange is accelerated by $10^3$ at the active site of RNR. The catalytic pathway for disulfide exchange, catalyzed by PDI has also been examined, and justification is given for why the major pathway for disulfide exchange should involve the release of PDI from the enzyme–substrate covalent complex by the active site protected cysteine ($C_{rescue}$). An additional role for the large hydrophobic PDI region has also been proposed, that is, to provide a hydrophobic environment to the folding substrate, thus catalyzing superficial disulfide rearrangement of non-native disulfide bonds. A mechanistic scheme for $S_N2$ reactions involving a concerted deprotonation/addition/protonation step mediated by the solvent has also been explored. In the system studied here, the mechanism results in a slightly slower reaction than the uncomplicated $S_N2$ reaction. The difference is, however, surprisingly and unexpectedly small. Thus such a scheme should not be excluded presently, as it is still unclear if it can be important in other $S_N2$ reactions involving weak bases, or under other experimental conditions.

## Acknowledgement

Fundação para a Ciência e Tecnologia (Project POCTI/35736/99, Portugal) and the National Foundation for Cancer Research (NFCR-U.S.A.) are gratefully acknowledged for financial support.

[1] H. F. Gilbert, *J. Biol. Chem.* **1997**, *272*, 29399
[2] R. J. Huxtable, *Biochemistry of Sulfur*, Plenum, New York, **1986**, p. 250.
[3] T. E. Creighton, P *rog. Biophys. Mol. Biol.* **1978**, *33*, 321
[4] H. F. Gilbert, *Methods Enzymol.* **1995**, *251*, 8.
[5] T. V. DeCollo, W. J. Lees, *J. Org. Chem.* **2001**, *66*, 4244.
[6] A. N. Glazer, E. L. Smith, *The Enzymes* Vol. III, 3rd ed. (Ed.: P. D. Boyer), Academic Press, New York, **1971**, p. 501.
[7] P. M. Weiss, R. J. Boerner, W. W. Cleland, *J. Am. Chem. Soc.* **1987**, *109*, 7201.
[8] S. Thompson, F. Mayerl, O. P. Peoples, S. Masamune, A. J. Sinskey, C. T. Walsh, *Biochemistry* **1989**, *28*, 5735.
[9] A. Holmgren, *Annu. Rev. Biochem.* **1985**, *54*, 237.
[10] J. Golik, J. Clardy, G. Dubay, G. Groenevold, H. Kawagushi, M. Konishi, H. Ohkuma, K. Saitoh, T. W. Doyle, *J. Am. Chem. Soc.* **1987**, *109*, 3461.
[11] G. L. Ellman, *Arch. Biochem. Biophys.* **1959**, *82*, 70.
[12] W. W. Cleland, *Biochemistry* **1964**, *3*, 480.
[13] G. M. Whitesides, J. E. Lilburn, R. P. Szajevski, *J. Org. Chem.* **1977**, *42*, 332.
[14] P. C. Jocelyn, *Methods Enzymol.* **1987**, *143*, 246.
[15] R. Singh, G. M. Whitesides, *J. Org. Chem.* **1991**, *56*, 2332.
[16] W. J. Lees, R. Singh, G. M. Whitesides, *J. Org. Chem.* **1991**, *56*, 7328.
[17] S. Ranganathan, J. Naraynaswamy, *J. Chem. Soc. Chem. Commun.* **1991**, 934.
[18] G. V. Lamoureux, G. M. Whitesides, *J. Org. Chem.* **1993**, *58*, 633.
[19] J. M. Wilson, R. J. Bayer, D. J. Hupe, *J. Am. Chem. Soc.* **1977**, *99*, 7922.
[20] R. Freter, E. R. Pohl, J. M. Wilson, D. J. Hupe, *J. Org. Chem.* **1979**, *44*, 1771.
[21] D. J. Hupe, D. Wu, *J. Org. Chem.* **1980**, *45*, 3100.
[22] R. P. Szajevski, G. M. Whitesides, *J. Am. Chem. Soc.* **1980**, *102*, 2011.
[23] J. Houk, G. M. Whitesides, *J. Am. Chem. Soc.* **1987**, *109*, 6825.
[24] T. V. DeCollo, W. J. Lees, *J. Org. Chem.* **2001**, *66*, 4244.
[25] W. Guo, J. Pleasants, D. Rabenstein, *J. Org. Chem.* **1990**, *55*, 373.
[26] D. Keire, E. Strauss, W. Guo, B. Noszál, D. Rabenstein, *J. Org. Chem.* **1992**, *57*, 123.
[27] D. Rothwarf, H. Scheraga, *Proc. Natl. Acad. Sci. USA* **1992**, 89, 7944.
[28] D. A. Kreire, E. Strauss, W. Guo, B. Noszál, D. L. Rabenstrin, *J. Org. Chem.* **1992**, *57*, 123.
[29] Gaussian 98, Revision A.9, M. J. Frisch, G. W. Trucks, H. B. Schlegel, G. E. Scuseria, M. A. Robb, J. R. Cheeseman, V. G. Zakrzewski, J. A. Montgomery, Jr., R. E. Stratmann, J. C. Burant, S. Dapprich, J. M. Millam, A. D. Daniels, K. N. Kudin, M. C. Strain, O. Farkas, J. Tomasi, V. Barone, M. Cossi, R. Cammi, B. Mennucci, C. Pomelli, C. Adamo, S. Clifford, J. Ochterski, G. A. Petersson, P. Y. Ayala, Q. Cui, K. Morokuma, D. K. Malick, A. D. Rabuck, K. Raghavachari, J. B. Foresman, J. Cioslowski, J. V. Ortiz, A. G. Baboul, B. B. Stefanov, G. Liu, A. Liashenko, P. Piskorz, I. Komaromi, R. Gomperts, R. L. Martin, D. J. Fox, T. Keith, M. A. Al-Laham, C. Y. Peng, A. Nanayakkara, M. Challacombe, P. M. W. Gill, B. Johnson, W. Chen, M. W. Wong, J. L. Andres, C. Gonzalez, M. Head-Gordon, E. S. Replogle, J. A. Pople, Gaussian, Inc., Pittsburgh PA, **1998**.
[30] A. D. Becke, *J. Chem. Phys.I* **1993**, *98*, 5648.
[31] C. Lee, W. Yang, R. J. Parr, *Phys. Rev. B.* **1998**, *37*, 785.
[32] R. W. Hertwig, W. Koch, *J. Comput. Chem.* **1995**, *16*, 576.
[33] P. A. Fernandes, M. J. Ramos, *J. Am. Chem. Soc.* **2003**, *125*, 6311.
[34] P. A. Fernandes, M. J. Ramos, *Chem. Eur. J.* **2003**, *9*, 5916.
[35] M. D. Lucas, P. A. Fernandes, L. A. Eriksson, M. J. Ramos, *J. Phys. Chem. B* **2003**, *107*, 5751
[36] V. Barone, M. Cossi, *J. Phys. Chem. A* **1998**, *102*, 1995.
[37] P. A. Fernandes, L. A. Eriksson, M. J. Ramos, *Theor. Chem. Acc.* **2002**, 108, 352.
[38] R. S. Mulliken, *J. Chem. Phys.* **1955**, *23*, 1833.
[39] B. H. Besler, K. M. , Jr. Merz, P. A. Kollman, *J. Comput. Chem.* **1990**, *11*, 431.
[40] U. C. Singh, P. A. Kollman, *J. Comput. Chem.* **1984**, *5*, 129.
[41] J. E. Carpenter, F. Weinhold, *Theochem* **1988**, 46, 41.
[42] A. E. Reed, R. B. Weinstock, F. Weinhold, *J. Chem. Phys.* **1985**, *83*, 735
[43] A. E. Reed, L. A. Curtiss, F. Weinhold, *Chem. Rev.* **1988**, *88*, 899.
[44] R. E. Rosenfield, R. Parthasarathy, J. D. Dunitz, *J. Am. Chem. Soc.* **1977**, *99*, 4860.
[45] L. Eldjarn, A. Pihl, *J. Am. Chem. Soc.* **1957**, *79*, 4589.
[46] K. H. Weaver, D. L. Rabenstein, *J. Org. Chem.* **1995**, *60*, 1904.
[47] W. J. Lees, G. M. Whitesides, *J. Org. Chem.* **1993**, *58*, 642.
[48] J. A. Pappas, *J. Chem. Soc. Perkin Trans. 2* **1979**, 67.
[49] M. Aida, C. Nagata, *Chem. Phys. Lett.* **1984**, *112*, 129.
[50] C. E. Grimshaw, R. L. Whistler, W. W. Cleland, *J. Am. Chem. Soc.* **1979**, *101*, 1521..
[51] M. Shipton, K. Brocklehurst, *Biochem. J.* **1978**, *171*, 385.
[52] H. Al-Rawi, K. A. Stacy, R. H. Weatherhead, A. William, *J. Chem. Soc. Perkin Trans. 2* **1978**, 663.
[53] N. Lambert, R. B. Freedman, *Biochem. J.* **1983**, *213*, 235.
[54] J. C. Edman, L. Ellis, R. W. Blacher, R. A. Roth, W. J. Ruter, *Nature* **1985**, *317*, 267.
[55] R. B. Freedman, H. C. Hawkins, S. J. Murant, L. Reid, *Biochem. Soc. Trans.* **1988**, *16*, 96.
[56] K. Vuori, R. Myllyla, T. Pihlajaniemi, K. Kivirikko, *J. Biol. Chem.* **1992**, *267*, 7211.
[57] R. Noiva, R. B. Freedman, W. J. Lennarz, *J. Biol. Chem.* **1993**, *268*, 19210.
[58] N. J. Darby, T. E. Creighton, *Biochemistry* **1995**, *34*, 16770.
[59] M. C. A. Laboissière, S. L. Sturley, R. T. Raines, *J. Biol. Chem.* **1995**, 270, 28006.
[60] K. W. Walker, M. M. Lyles, H. F. Gilbert, *Biochemistry* **1996**, *35*, 1972.
[61] H. F. Gilbert, *J. Biol. Chem.* **1997**, *272*, 29399.

  

[62] K. W. Walker, H. F. Gilbert, *J. Biol. Chem.* **1997**, *272*, 8845.
[63] J. Zheng, H. F. Gilbert, *J. Biol. Chem.* **2001**, 276, 15747.
[64] T. E. Creighton, D. A. Hillson, R. B. Freedman, *J. Mol. Biol.* **1980**, *142*, 43.
[65] P. Klappa, L. W. Ruddock, N. J. Darby, R. B. Freedman, *EMBO J.* **1998**, *17*, 927.
[66] J. Stubbe, W. A. van der Donk, *Chem. Rev.* **1998**, *98*, 705.
[67] R. Prabhakar, M. R. A. Blomberg, P. E. M. Siegbahn, *Theor. Chem. Acc.* **2000**, 104, 461..

Received: July 16, 2003 [F5343]